Cytotoxic immunological synapses do not restrict the action of interferon-γ to antigenic target cells

Nicholas Stephen Rennie Sanderson[a,b], Mariana Puntel[b], Kurt M. Kroeger[b,2], Niyati S. Bondale[b], Mark Swerdlow[b], Niloufar Iranmanesh[b], Hideo Yagita[c], Ahmed Ibrahim[b], Maria G. Castro[a,b], and Pedro R. Lowenstein[a,b,1]

[a]Department of Neurosurgery and Department of Cell and Developmental Biology, The University of Michigan Medical School, Ann Arbor, MI 48109; [b]Board of Governors' Gene Therapeutics Research Institute, Cedars-Sinai Medical Center, Los Angeles, CA 90048; and [c]Department of Immunology, Juntendo University, Tokyo 113-8421, Japan

Edited by Michael L. Dustin, Skirball Institute of Biomolecular Medicine, New York, NY, and accepted by the Editorial Board April 3, 2012 (received for review September 29, 2011)

Following antigen recognition on target cells, effector T cells establish immunological synapses and secrete cytokines. It is thought that T cells secrete cytokines in one of two modes: either synaptically (i.e., toward antigenic target cells) or multidirectionally, affecting a wider population of cells. This paradigm predicts that synaptically secreted cytokines such as IFN-γ will preferentially signal to antigenic target cells contacted by the T cell through an immunological synapse. Despite its physiological significance, this prediction has never been tested. We developed a live-cell imaging system to compare the responses of target cells and nonantigenic bystanders to IFN-γ secreted by CD8+, antigen-specific, cytotoxic T cells. Both target cells and surrounding nontarget cells respond robustly. This pattern of response was detected even at minimal antigenic T-cell stimulation using low doses of antigenic peptide, or altered peptide ligands. Although cytotoxic immunological synapses restrict killing to antigenic target cells, the effects of IFN-γ are more widespread.

astrocyte | two-photon microscopy | Stat1 | neuroimmunology | adenoviruses

When cytotoxic T cells encounter cells displaying their cognate antigens, they respond with two effector mechanisms: secretion of cytokines and lysis of target cells. T cells possess mechanisms to restrict killing to antigenic cells; i.e., immunological synapses confine delivery of lytic granules to target cells (1). Cytokine secretion has a wider potential field of influence. It has been proposed that individual cytokines can either be secreted directly onto the antigenic target cell in a way analogous to the focused release of lytic granules, or alternatively be secreted in a diffuse manner affecting both the T cell's antigenic target and bystander cells.

The spatial dynamics of cytokine secretion were first investigated to understand how a soluble, secreted signaling molecule mediates an antigen-specific (and therefore cell-to-cell) interaction. In the late eighties, Janeway's group (2) demonstrated that T helper cells stimulated by low levels of anti-TCR antibody preferentially released IL-4 in the direction of the stimulus. The authors proposed that "polar release" contributes to the ability of helper T cells to activate only those B cells with which they shared antigen specificity.

This concept was developed further by the Kupfer group. In conjugates of helper T cells and antigen-presenting B cells, IL-2, IFN-γ, IL-4, and IL-5 were all localized at the microtubule organizing center (MTOC), in the area of the T cell apposed to the B cell (3). The authors proposed that this polarized cytokine production was involved in the antigen-specific activation of B cells (4).

Intracellular distributions of several cytokines have been examined quantitatively in helper T cells following interaction with antigen-presenting B cells or with antigenic surfaces (5). These studies confirmed the polarization of IFN-γ and IL-2 toward the antigen-presenting cells (APC). Other cytokines, e.g., tumor necrosis factor (TNF) and IL-4, were localized more diffusely throughout T cells. TNF was secreted multidirectionally without regard for the location of the APC. The authors described these two routes of secretion as "synaptic" and "multidirectional," and proposed that they represent fundamentally distinct intracellular secretory pathways with distinct physiological consequences (5, 6). This two-pathway model is depicted in Fig. 1. Few attempts have been made to test functional predictions of this model in vivo. However, Perona-Wright et al. (7) examined response to IL-4 in reactive lymph nodes during helminth infection and found that it was not limited to discrete antigenic targets. IFN-γ signaling during *Toxoplasma* infection was similarly ubiquitous. Because each of these cytokines has been postulated to be secreted in a synaptically restricted pattern in vitro (3, 5), these results raise the possibility that synaptically secreted cytokines may exert their effects beyond the target cell.

During immune-mediated clearance of virally infected cells from the brain, CD8+ cytotoxic T lymphocytes (CTLs) form immunological synapses with virally infected cells (8). In these CTLs, IFN-γ is polarized toward the antigenic target cell (9). According to the two-pathway model, polarized distribution of cytokines implies polarized secretion and cytokine signaling restricted to the target APC. Because the physiological consequences of the pattern of cytokine secretion are determined by the population of responding cells, rather than by the intracellular distribution of cytokines, we examined directly whether response to IFN-γ signaling is restricted to antigenic targets.

We set up a live-cell imaging system in which the responses to IFN-γ in antigenic targets and nonantigenic "bystanders" were monitored during the course of T cell/target cell interactions. Responses we observed did not fall discreetly into either the "synaptic" or "multidirectional" pattern. As CD8+ T cells interacted with astrocytes, target cells responded earlier and more strongly, but nontarget bystander cells also responded robustly. Using a fixed-cell preparation with minimal levels of antigenic stimulation, we also observed responses in nonantigenic bystanders. These results suggest that even if IFN-γ is secreted by CD8+ CTL in a synaptically polarized manner, it diffuses from the synapse and signals to neighboring nonantigenic cells. Cytotoxic immunological synapses, although efficiently restricting killing to target cells, do not restrict cytokine signaling.

Author contributions: N.S.R.S., M.G.C., and P.R.L. designed research; N.S.R.S., M.P., K.M.K., N.S.B., M.S., N.I., and A.I. performed research; H.Y. contributed new reagents/analytic tools; N.S.R.S., M.G.C., and P.R.L. analyzed data; and N.S.R.S., M.G.C., and P.R.L. wrote the paper.

The authors declare no conflict of interest.

This article is a PNAS Direct Submission. M.L.D. is a guest editor invited by the Editorial Board.

[1]To whom correspondence should be addressed. E-mail: pedrol@umich.edu.

[2]Deceased November 25, 2011.

This article contains supporting information online at www.pnas.org/lookup/suppl/doi:10.1073/pnas.1116058109/-/DCSupplemental.

IMMUNOLOGY

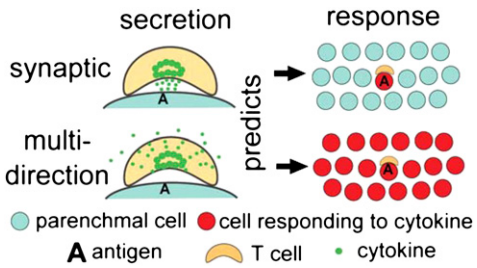

Fig. 1. Two-pathway model of cytokine secretion by effector T cells responding to antigen. In the synaptic pathway (*Upper*) cytokine is secreted into the synaptic cleft and its effects are focused on the target cell by the immunological synapse. At the tissue level (schematized *Upper Right*) the postulated functional consequence of this pattern of secretion is that antigenic targets will receive stronger cytokine signaling than nonantigenic "bystanders". In the multidirectional pathway (*Lower*), once the T cell is activated by antigenic stimulation from the target cell, cytokine is secreted nondirectionally, At the tissue level (*Lower Right*), this will result in widespread cytokine signaling to nearby cells.

Results and Discussion

Stat1-Cherry Imaging Enables Real-Time Monitoring of IFN-γ Action. We set up a live-cell imaging system in which response to IFN-γ was visualized by tracking the intracellular localization of a Stat1-cherry fusion protein (see Fig. 2). Without IFN-γ, this fusion protein is predominantly cytoplasmic, and with exposure to IFN-γ, translocates into the nucleus (Fig. S1*A* and Movie S1). Stat1-cherry translocation is dose-dependent, with concentrations of IFN-γ greater than 10 pg/mL inducing graded increases of nuclear Stat1-cherry fluorescence. This response is IFN-γ specific because Stat1-cherry translocation is prevented by anti-IFN-γ blocking antibodies, as is the phosphorylation of endogenous Stat1 (Fig. S2 *B* and *C*).

Target Cells and Nontarget Cells Respond to IFN-γ. According to Huse et al. (5, 6), "synaptic" secretion has the following experimentally measureable characteristics: (*i*) intracellular location of the cytokine apposed to the synapse and the MTOC, and association with a particular set of intracellular trafficking proteins; and (*ii*) nocodazole-sensitive tightly focused cytokine spots in 2D capture assays. In view of these characteristics, Huse et al. proposed: (*iii*) that the cytokine is secreted into the synaptic space (and constrained therein); and (*iv*) that the synaptically secreted cytokine would therefore preferentially stimulate the antigenic target cell. To test this critical fourth hypothetical characteristic in the context of CTL attack, we compared the response to IFN-γ action in targets versus bystander cells. A few antigenic target cells were seeded among a large number of nonantigenic bystanders and the coculture induced to express Stat1-cherry via an adenoviral vector. The distinction between targets and nontargets was achieved through MHC matching (C57BL/6, K^b) or mismatching (BALB/c, K^d) to the OT-I specificity, and further by infecting only the targets with an adenoviral vector encoding a fusion protein containing SIINFEKL, the epitope recognized by OT-I cells. This fusion protein also included influenza nucleoprotein, which targeted the protein to the nuclei, and GFP, which distinguished target from nontarget cells (see Fig. 2). Responsiveness of "targets" and "non-targets" to recombinant IFN-γ was compared, and the two cell populations responded similarly (Fig. 2*L*).

Activated CD8+ OT-I T cells were added to these cocultures and within 2–8 h of the T cells establishing contact with targets, Stat1-cherry translocation was observed with a time course comparable with that induced by exogenous IFN-γ (Fig. 3); in the absence of OVA expression by target cells, there was no production of IFN-γ by T cells (Fig. S3*G*). In a typical time series (see Movies S2 and S3), T cells added to the medium were first

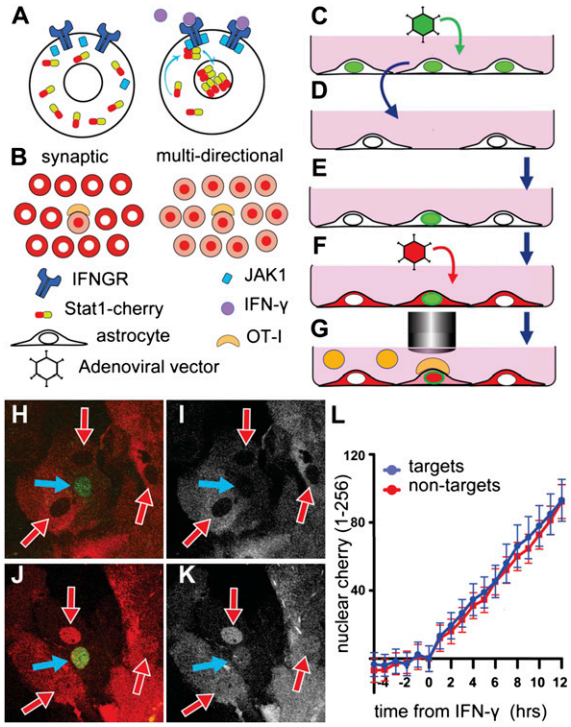

Fig. 2. (*A*) Stat1-cherry reporter system. Before exposure to IFN-γ, Stat1 is localized in the cytoplasm (*Left*). With IFN-γ bound to the IFN-γ receptor (IFNGR), a complex is formed involving the phosphorylation of the Janus Kinase 1 (Jak1), and the transcription factor Stat1 (*Right*). Thus, phosphorylated, Stat1 translocates into the nucleus and mediates the transcription of IFN-γ–responsive genes. Stat1-cherry translocates similarly, and its localization can be followed by measuring cherry fluorescence in the nucleus. (*B*) IFN-γ signaling by the synaptic and multidirectional pathways depicted in Fig. 1 will result in distinct patterns of Stat1-cherry translocation when T cells interact with isolated antigenic targets among nonantigenic bystanders. Synaptic signaling (*Left*) will induce translocation preferentially in the target, whereas multidirectional signaling (*Right*) will result in widespread, antigen-indiscriminate translocation. (*C–G*) experimental procedure. (*C*) K^b-expressing C57 astrocytes are infected with an adenoviral vector mediating expression of a SIINFEKL-NP-GFP fusion protein, and then immediately trypsinized. (*D*) Small numbers added to an almost-confluent monolayer of K^d-expressing (i.e., MHC mismatched) BALB/c astrocytes. The coculture (*E*) is then superinfected (*F*) with a second adenoviral vector encoding Stat1-cherry. Once expression of both transgenes is verified, the coculture is imaged for several hours in a controlled environment under a two-photon microscope (*G*), and once baseline cherry levels are established, activated T cells are added. Images are captured from 20 to 60 locations, each containing at least one target cell, and also from at least one location with no target cells, over 12–36 h. These images are then postprocessed to analyze the pattern of translocation. (*H–L*) Results from a control experiment using exogenous recombinant IFN-γ instead of T cells to induce uniform translocation in all cells. (*H*) A target cell (green nucleus indicated by blue arrow) surrounded by nontarget cells (indicated with red and white arrows), all expressing Stat1-cherry, before addition of IFN-γ. The red channel from this image is shown in *I* and reveals that before IFN-γ addition, cherry fluorescence is predominantly cytoplasmic. (*J*) Image captured at the same location 8 h after IFN-γ addition. In the cherry-only image from this location (*K*), it is clear that Stat1-cherry has translocated into the nucleus, both in the target (blue arrows in *H–K*), and in the other cells (red and white arrows in *H–K*), most clearly in the neighboring nontarget just above the target (see also Movie S1). In this experiment, images were captured from 24 locations, of which 6 were rejected because of imaging artifacts such as bubble formation. For the remaining 18 locations, nuclear cherry fluorescence (encoded from 0 = threshold of detection to 256 = saturation) was measured over time for one "target" and one nearby "non-target", and the data for the two kinds of cell averaged at each time point to produce the plots in *L*. The blue line represents nuclear cherry fluorescence over time in the "target" nuclei, and the red line that in "non-target" nuclei. (Note that in the absence of T cells, the distinction between "targets" and "non-targets" is purely nominal.) This control live-cell imaging experiment was repeated three times.

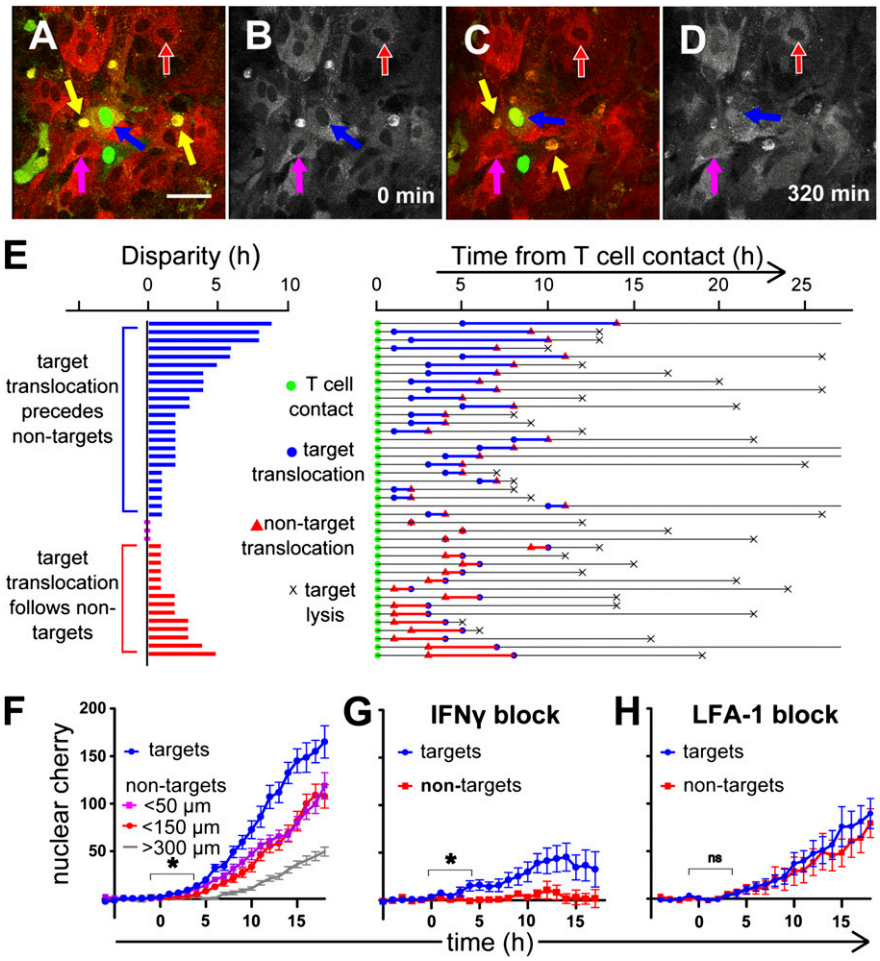

Fig. 3. Live cell imaging of interactions between T cells, targets, and nontargets. Activated OT-I T cells labeled with PKH-26 (yellow arrows in *A* and *C*) were added to a monolayer of astrocytes, including a small number of antigenic targets (C57BL/6 astrocytes infected with Ad.OVA-NP-GFP) among a majority of nontargets (BALB/c astrocytes). Both target and nontarget astrocytes express the Stat1-cherry fusion protein (red) from an adenoviral vector. (*A* and *C*) Frames taken at the point of T-cell contact, and then 320 min later from a single location containing two target cells (green nuclei, indicated by blue arrows), and >30 nonantigenic bystanders. (Scale bar: 40 μm.) (*B* and *D*) The same images as *A* and *C* with the green channel removed to reveal the intensity of cherry fluorescence in the nuclei. Until T-cell contact (*B*), red fluorescence from the Stat1-cherry fusion protein is cytoplasmic. After T-cell contact, in those astrocytes that respond to IFN-γ from T cells stimulated by antigenic targets, Stat1-cherry translocates into the nuclei. This is seen most clearly in the cherry-only channel 320 min after contact (*D*); at this location the strongest translocation is seen in the target cell (see also Movie S2). (*E*) Relative response times of targets and nontargets to IFN-γ. Time lines were plotted for each location (right side), with the point of T-cell contact at the beginning of the line (green circle); and the time at which each cell showed Stat1-cherry translocation (i.e., nuclear cherry fluorescence exceeded 3 SDs above baseline mean) plotted with a blue circle (targets), or a red triangle (adjacent nontargets). The point at which the target cell was lysed is represented with a black cross. The horizontal axis represents the time after T-cell contact, and time lines for 41 locations, pooled from two similar experiments are arranged down the vertical axis. The bar chart on the left shows the difference (nontarget cell translocation latency − target cell translocation latency) represented as horizontal bars, for the same 41 cells, arranged top to bottom from greatest (i.e., target cell translocates longest before nontarget) to least (i.e., target cell translocates longest after nontarget). For these 41 pairs of targets and nontargets, the translocation times were subjected to a paired, two-tailed, Student *t* test, revealing that target translocation (mean latency = 4.0 h from T-cell contact) is significantly faster than nontarget translocation (mean latency = 5.2 h, $P = 0.02$). (*F*) Average time course of translocation. Images are captured at 20-min intervals from each location on the monolayer. Postcapture, the images are analyzed by measuring the nuclear cherry fluorescence in targets (blue arrows in *A–D*, blue line in *F*), adjacent nontargets in the same field of view as the target (<50 μm from target; average 30 μm; magenta arrows *A–D*; magenta line in *F*), more distant nontargets in the same field of view (<150 μm from target, average 80 μm; red and white arrows in *A–D*; red line in *F*), and nontargets in a distant field of view containing no targets (separated by >300 μm from the nearest target; gray line in *F*). Each point is the grand mean (±SEM) from the 41 locations shown in *E*. The asterisk indicates that over the 6 h from just before T-cell contact to 4 h after, the time course of translocation in targets is significantly different from that in adjacent nontargets (repeated measures two-way ANOVA, interaction between time and group $P = 0.0438$). (*G*) Data from an experiment similar to that shown in *F*, other than that before the addition of T cells, a monoclonal rat anti-mouse IFN-γ antibody was added at 10 μg/mL to block IFN-γ action. Only targets (blue line) and nearby nontargets (red line) were measured. The asterisk indicates that over the 6 h from just before T-cell contact to 4 h after, the time course of translocation in targets is significantly different from that in nearby nontargets (repeated measures two-way ANOVA, $P = 0.0412$). Likewise, in the experiment whose results are shown in *H*, an LFA-1 blocking antibody was added at 10 μg/mL before the T cells. Again, only targets (blue line) and nearby nontargets (red line) were tracked. The letters "ns" indicate that, over the 6 h from just before T-cell contact to 4 h after, the time course of translocation in targets is not significantly different from that in adjacent nontargets (repeated measures two-way ANOVA, $P = 0.9849$). The basic experiment on which *A–F* are based was repeated six times, and the experiments with blocking antibodies were repeated once each.

observed on the monolayer of targets and nontargets at a location not contacting the target. T cells apparently adhered to the monolayer, and moved around in a locus larger than the field of view, until contact was made with an antigenic target. Not every T cell remained in contact with the target, but typically, once contact was made the movements of the T cell were restricted to the target. During the following hours of imaging, three phenomena were recorded quantitatively. First, Stat1-cherry translocation was observed (Movie S2). Second, additional T cells accumulated at the site at an average rate of approximately one every 3 h (Fig. S3). Third, lysis of the target cell was observed, as inferred from morphological distortion, membrane blebbing, and disintegration (see Movie S3). Lysis of nontarget cells was not observed. Typically, Stat1-cherry translocation occurred while one to three T cells were in contact with the target (Fig. S2*F*). By contrast, lysis was only observed after at least three T cells had accumulated (Fig. S3*F*), often immediately after being contacted by an additional T cell (Movie S3). Lysis usually occurred several hours after Stat1 translocation, which is longer than is typical for T-cell–mediated lysis of transformed B cells (10), but consistent with other studies using nonhematopoetic cells as targets (11, 12). Accumulations of recruited T cells generally persisted after the death of the target cell until the end of the imaging period (Movie S3). To determine whether IFN-γ secretion continues after target lysis, we compared the slopes of translocation curves of individual bystander cells before and after the lysis of the target. Rates of translocation were indistinguishable before and after target lysis, suggesting that IFN-γ secretion continues after

target lysis (Fig. S4), consistent with results from Valitutti's group (10). To assess the level of antigen-independent IFN-γ secretion by activated OT-I T cells, a control assay was run using the same cocultures of BALBc astrocytes as bystanders and C57BL/6 astrocytes as "targets," but in this case the Ad.ckOVA-NP-GFP vector was replaced with an adenoviral vector encoding GFP alone. When such cocultures were pulsed with 100 pM SIINFEKL before adding OT-I T cells, the results were similar to those seen with Ad.ckOVA-NP-GFP-infected C57BL/c astrocytes, but when the pulsing was omitted, Stat1-cherry translocation was similar to the level seen without T cells (Fig. S1*B*).

The synaptic model of secretion predicts that response to IFN-γ (i.e., Stat1-cherry translocation) will initially be limited to the "post-synaptic" antigenic target cells. The multidirectional model predicts that all cells in the vicinity of a T-cell/target-cell interaction ought to respond equally. Time course and intensity of translocation differed from either prediction. At every location, both target and nontarget cells translocated, and the order was variable (Fig. 3*E*). At 24 of 41 locations, the target cell translocated before the nontarget (up to 8 h earlier); at 3 locations, target and nontarget translocated simultaneously; and at 14 of 41 locations, the nontarget cell translocated first (up to 5 h earlier). On average, Stat1-cherry translocation was detectable earlier in targets than in nontarget cells: Mean target cell translocation occurred at 4 h after T-cell contact, nontarget cells within 150 μm of target cells had a mean translocation latency of 5.2 h, and nontarget cells >300 μm away had a mean translocation latency of 9.5 h. Translocation was also weaker on average in nontarget cells: Nontarget cells within 150 μm displayed a mean nuclear cherry intensity at 10 h of 64% of that seen in targets, and nontarget cells >300 μm from target cells displayed a relative intensity of 15% (Fig. 3*F*).

Stat1-Cherry Translocation Pattern Depends on IFN-γ and LFA-1. The relationships between immunological synapse formation, IFN-γ signaling and Stat1-cherry translocation were probed further using blocking antibodies. Adding a monoclonal antibody against IFN-γ to an astrocyte monolayer before adding recombinant IFN-γ abolished nuclear accumulation of phosphorylated Stat1 (Fig. S2*B*). Adding this antibody to a coculture of target and nontarget cells before adding OT-I T cells completely eliminated translocation in nontarget cells (Fig. 3*G* and Fig. S2*C*). The extent of translocation was greatly reduced in target cells (Fig. 3*G*), although the number of cells translocating was not reduced significantly (Fig. S1*D*), possibly because the structure of the immunological synapse offers a partial barrier to antibody entry. An alternative possibility is that some process induced in the target cells by T-cell attack might result in target-specific, IFN-γ-independent Stat1-cherry translocation.

T-cell adhesion depends on the integrin Lymphocyte Function-Associated Antigen 1 (LFA-1) (13), and this adhesion molecule is also involved in the formation of immunological synapses between CD8+ CTLs and target astrocytes (8). Addition of a blocking antibody to LFA-1 resulted in a diminished overall response and eliminated the difference between targets and nontargets (Fig. 3*H*), suggesting that the difference between target and nontarget cells seen in Fig. 3*F* is due to the LFA-1–dependent properties of the immunological synapse. This loss of restriction is reminiscent of the diminution of CTL cytotoxicity with impaired focusing of CTL lytic granules onto target cells following disruption of the peripheral SMAC by LFA-1 blocking antibodies (14).

T-Cell Signaling to Nontarget Cells Is Independent of Antigenic Signal Strength: Results with Low Levels of SIINFEKL and Altered Peptide Ligands. Because the polarized release reported by the Janeway group was only observed at low levels of TCR stimulation, we investigated the possibility that the absence of synaptic restriction in our live-cell imaging paradigm was due to strong signaling at the OT-I TCR. To control the level of antigenic stimulation, we pulsed astrocytes with increasing concentrations of the canonical OT-I epitope SIINFEKL and two altered peptide ligands, SIIGFEKL and EIINFEKL, which have been demonstrated to mediate respectively intermediate and low signaling at the OT-I TCR (15). After washing, cocultures of astrocytes and OT-I T cells were incubated for 6 h, fixed, and immunolabeled for IFN-γ, LFA-1 and phosphorylated Stat1.

The number of adherent T cells increased with increasing concentration of peptide; the maximum number of T cells was reached with 100 pM SIINFEKL (Fig. 4*A*). The percentage of IFN-γ immunoreactive OT-I cells, and the number of responding astrocytes also increased with SIINFEKL concentration (Fig. 4*B*). No concentration of EIINFEKL induced a significant increase in T-cell IFN-γ or astrocyte pStat1 immunoreactivity. In astrocytes pulsed with the highest dose of 1 μM SIIGFEKL we were able to detect nuclear pStat1 (Fig. 4*C*), although in line with previous reports (16) we did not find reliable immunolabeling for IFN-γ in T cells, suggesting that the Stat1 phosphorylation we observed was induced by a level of IFN-γ too low to detect immunocytochemically.

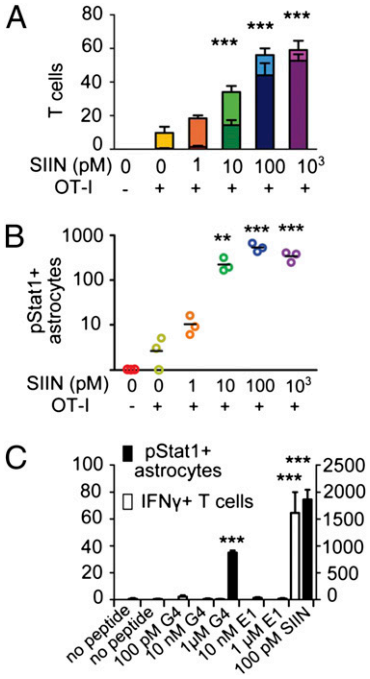

Fig. 4. The effect of reduced antigenic stimulus. (*A* and *B*) Astrocytes from C57BL/6 pups cultured on glass coverslips were pulsed with various concentrations of the canonical OT-I epitope SIINFEKL (SIIN), before coculture with activated OT-I T cells, fixation, and fluorescent immunolabeling for IFN-γ, LFA-1, and phospho-Stat1. Immunoreactive cells were then counted in 15–20 semirandomly placed fields per coverslip under 20× objective using a fractionator routine. (*A*) For the indicated combinations of T cells and peptide concentration, the number of T cells (LFA-1 immunoreactive, lighter colored bars) and the number of those T cells that were coimmunolabeled for IFN-γ (superimposed darker colored bars). Data are shown as means of triplicates with SEM. (*B*) The number of phospho-Stat1 immunoreactive astrocytes in the same counting areas. Individual data points are plotted. Data were subjected to Kruskal-Wallis test to confirm differences between group medians, and then to one-way ANOVA. (**$P < 0.01$; ***$P < 0.001$). (*C*) Results of a similar experiment used to assess the antigenic potential of various combinations of two altered peptide ligands, EIINFEKL and SIIGFEKL. Empty bars show number of IFN-γ immunoreactive T cells counted in each condition, including a positive control in which astrocytes were pulsed with 100 pM SIINFEKL, and duplicates for the positive control. Solid bars show numbers of phospho-Stat1 immunoreactive astrocytes in the same counting areas. Bars show means and error bars SEM. Statistics as in *A* and *B*.

We used low concentrations of SIINFEKL and various concentrations of the altered peptide ligands to pulse mixed monolayers of targets and nontargets like those used for live-cell imaging studies. After coculture and fixation, we immunolabeled them for LFA-1, IFN-γ, and pStat1. Targets were distinguished from nontargets by labeling with Qtracker-655 quantum dots. At high concentrations of SIINFEKL (>100 pM), Stat1 phosphorylation was essentially ubiquitous. At the lowest effective concentration of SIINFEKL (10 pM) or SIIGFEKL (1 μM), Stat1 phosphorylation was found in both targets and surrounding nontarget cells, forming "patches" of pStat1 immunoreactive cells with targets at their centers (Fig. 5 *A–E*). No concentration of antigenic peptide resulted in pStat1 immunoreactivity exclusively in antigenic target cells.

To assess the possibility that target-restricted IFN-γ action might be seen at earlier time points, we repeated the experiment with 10 or 100 pM SIINFEKL, 1 μM SIIGFEKL, or no pulsing and fixed the cocultures at 1, 2, 3, or 4 h. Without pulsing, no patches were observed, and at 1 h only one small patch was observed in the 100 pM SIINFEKL condition. With increasing antigenic strength or increasing time, patches of greater size (greater numbers of pStat1 immunoreactive bystanders per patch) were observed, but no pStat1 immunoreactive target unaccompanied by activated bystanders was ever observed (Fig. 5*F*).

Within these patches, nuclear pStat1 immunofluorescence was greatest in bystanders close to the target, and diminished with distance (correlation of distance from target with pStat1 immunofluorescence: $R^2 = 0.1520$, $n = 917$, $P < 0.0001$), consistent with the hypothesis that IFN-γ is released at the T-cell/target interaction and diffuses outwards.

To assess whether the preferential activation shown by target cells in our live-cell imaging paradigm should be ascribed to synaptically focused IFN-γ secretion, or simply to the effect of proximity, we used the nocodazole paradigm developed by Huse et al. (5). After allowing 1 h for T cells to form contacts with targets, we added 33 μM nocodazole to disrupt microtubules and interfere with synaptic signaling. We then compared the ratio of pStat1 immunofluorescence in targets and surrounding bystanders. Without nocodazole, the ratio was 1.9:1, and with nocodazole treatment was 1.3:1 (two-tailed *t* test, $P = 0.0251$), suggesting that synaptic signaling contributes to the preferential activation of target cells (Fig. 5 *G* and *H*).

Immunolabeling fixed cocultures also enabled us to visualize the intracellular location of IFN-γ in the T cells. As others have

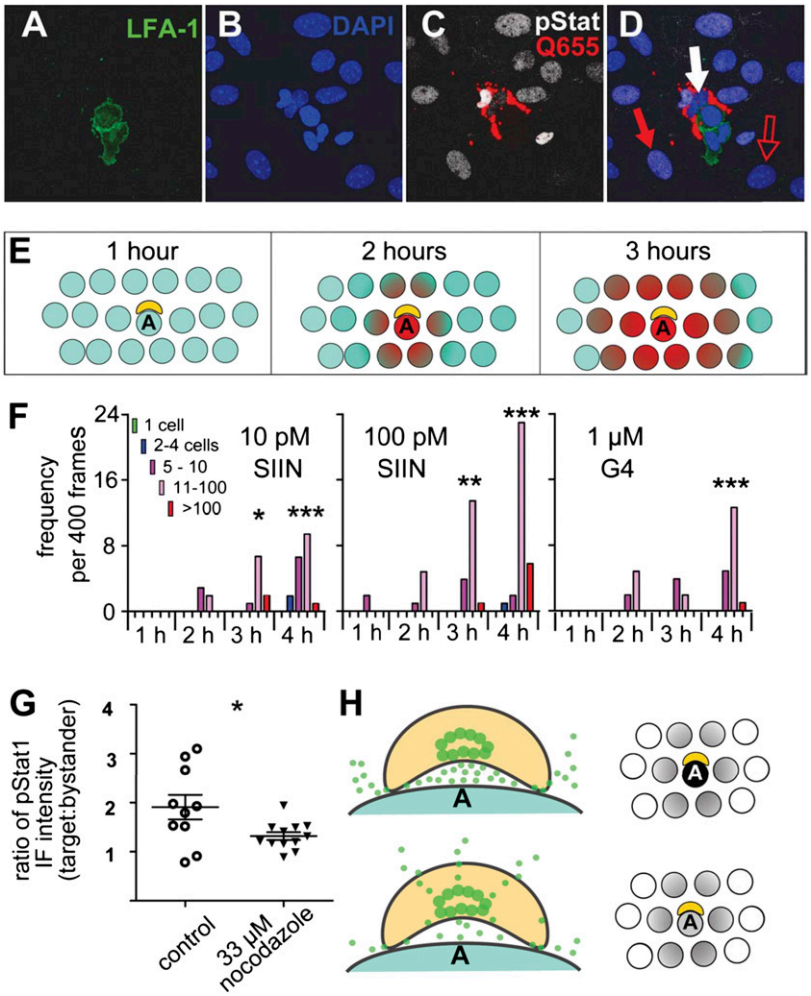

Fig. 5. Response to IFN-γ secreted during graded antigenic stimulation. (*A–D*) Patch of pStat1-immunoreactive bystander cells surrounding a target cell/T-cell contact. Cultures of 50,000 unlabeled BALB/c astrocytes (MHC-mismatched, nontargets) containing 500 Qtracker655-labeled C57BL/6 astrocytes (MHC-matched targets) were pulsed with 10 pM SIINFEKL and then cocultured with activated OT-I T cells. After 6 h, these cocultures were fixed and immunolabeled for IFN-γ, LFA-1, and phospho-Stat1. (*A*) LFA-1 (T cells, green). (*B*) DAPI (nuclei of all cells, blue). (*C*) Qtracker 655 (C57 targets, bright red in center of field), merged with phospho-Stat1 (cells responding to IFN-γ, white nuclei). (*D*) All four channels merged. In addition to the antigenic target cell (white arrow), examples are indicated in *D* of a cell in which phospho-Stat1 labeling indicates that the cell responded to IFN-γ signaling (solid red arrow), and one in which labeling is below detection (outlined red arrow). (*E*) Schematic depiction of relationship between patch size and length of T-cell/target interaction, based on data shown in *F*. (*F*) Frequencies of patches of various sizes as a function of antigenic strength and time. Cocultures as described in *A–D* (but with target cells labeled with Cell tracker Green, rather than Q655) were pulsed with 10 pM SIIN, 100 pM SIIN, 1 μM G4, or unpulsed, and then fixed 1, 2, 3, or 4 h after T-cell addition and immunolabeled for pStat1. Coverslips were examined at counting frames placed semirandomly by a computer on a 600 μM grid and the presence or absence of a patch (cluster of pStat1+ cells surrounding a pStat1+ target cell) recorded. When found, the number of pStat1+ bystanders was recorded. Without peptide pulsing, no patches were observed at any time point. At 1 h, no patches were observed except a single example in the 100 pM SIIN condition. From 2 h onwards, numerous patches were observed, increasing in size and number, as shown. No instance was observed of a translocated pStat1+ target cell unaccompanied by pStat1+ bystanders. (*$P < 0.05$; **$P < 0.01$, ***$P < 0.001$ v. 1h time-point; Kruskal-Wallis test, followed by Dunnett's test). (*G*) Effect of nocodazole treatment on preferential activation of target cells. Cocultures as described in *F* were treated with 33 μM nocodazole or control at 1 h after addition of T cells and then 2 h later fixed and immunolabeled for pStat1. Coverslips were examined for patches and when found these were imaged at 40× magnification. These images were analyzed with ImageJ to measure intensity of pStat1 immunofluorescence in targets and bystanders, and the ratio plotted on this column scatter graph. The target:bystander ratio was ~1.9:1 in control patches and 1.3:1 in nocodazole treated patches ($P = 0.0251$; unpaired, two-tailed *t* test). (*H*) The leaky synaptic model of cytokine secretion by T cells. According to the two-pathway model (see Fig. 1), cytokines can be secreted either synaptically or multidirectionally. Our results are compatible with a model in which IFN-γ secretion is synaptic, but leaks from the synapse to stimulate nearby cells. Treatment with nocodazole disrupts the synaptic component and yields a pattern of cytokine action compatible with multidirectional secretion.

IMMUNOLOGY

observed in helper T cells in culture (3, 5) and we have observed in CD8+ CTL in vivo (9), IFN-γ can be seen as an intense focus of immunolabeling surrounding a tubulin-rich core, presumably the MTOC, and this whole assembly is found on the side of the T cell that appears to be intimately contacting the antigen-presenting target cell (Fig. S5), but a sparser population of IFN-γ-immunoreactive puncta are also observed throughout the cytoplasm.

For five main reasons, we interpret these results as implying a leaky synaptic pattern of IFN-γ secretion, as depicted in Fig. 5*H*. First, the response observed consistently in nonantigenic bystander cells is incompatible with complete restriction of cytokine secretion by cytotoxic immunological synapses. Second, the intracellular synaptic polarization of IFN-γ is consistent with secretion of the cytokine at the immunological synapse. Third, the observation that IFN-γ blocking antibodies eliminate responses in nontarget cells, whereas targets display a residual response, is consistent with secretion of cytokine into the immunological synapse and its subsequent diffusion out of the synapse. Fourth, the effect of LFA-1 antibodies in reducing the differences in responses between targets and bystander cells also supports synaptic secretion. Finally, the diminution of preferential target cell response following nocodazole treatment is consistent with synaptically directed IFN-γ secretion. In our paradigm, it would be possible that permeability changes induced by cytolytic factors secreted by CTL cells may affect the function of immunological synapses.

Previous relevant experimental results mostly concern noncytotoxic, CD4+ T cells, but we note that some of these observations could also be explained by the leaky synaptic paradigm. Kupfer and collaborators (4) demonstrated polarized IL-4 secretion by T helper cells, but noted that nonantigenic bystander B cells also proliferate, albeit with a delay. Perona-Wright et al. (7) found that signaling by IFN-γ, a synaptically secreted cytokine (5), was essentially ubiquitous throughout the reactive lymph node. Our results enable us to reconcile the apparent multidirectional effects of synaptically released cytokines described in vivo (7). This thesis predicts that in the brain in vivo the actions of synaptically released IFN-γ from CTL will also extend to nonantigenic cells. A comparison of the potential leakiness of cytokines and cytotoxic granules released by CD4 and CD8 T cells (17), and how the kinetics of immunological synapses (18) influence the precise delivery of T-cell effectors to target cells remains to be explored in the future.

Lack of restriction of cytokine action remains compatible with a polarized pattern of secretion: In neural synapses, neurotransmitters are secreted synaptically but rapidly diffuse out of the synaptic cleft, and other mechanisms are required to restrict their action to the synapse (19). We note that although the action of IFN-γ is not synaptically restricted in our system, cytotoxic lysis is confined to antigenic targets. This distinction may reflect a difference in the permeability of the synaptic seal to cytokines versus lytic granules, or a difference in the properties of the secreted products; IFN-γ is stable and active at low concentrations in extracellular media, while isolated lytic granules have very weak lytic capacity (20). It is conceivable that cytolytic factors secreted by CTL might increase the permeability of immunological synapses to IFN-γ. However, as in many cases, nuclear Stat1 translocation in nontargets precedes death of target cells by as much as 12 h, and in some cases cell death is not detected, we believe that cytotoxicity induced leakage is unlikely to be the main determinant of our results.

There is strong evidence that certain cytokines, including IFN-γ, are secreted by T cells in a polarized fashion toward the immunological synapse. This result suggests that the effect of such cytokines might be restricted to the "post-synaptic" antigenic target cells. Our work indicates that, at least for cytotoxic T cells, IFN-γ signaling is not completely restricted by the immunological synapse. During viral infections of the brain, only infected cells express antigenic targets for CTLs, and so a wider sphere of IFN-γ action may serve to activate widespread protective antiviral mechanisms throughout the infected brain.

Methods

Procedures involving live animals were reviewed and approved by Cedars Sinai Medical Center's Institutional Animal Care and Use Committee (Animal Welfare Assurance A3714-01), or the University of Michigan Committee on Use and Care of Animals. Efforts were made throughout to minimize consumption of energy and disposables. Detailed methods are described in *SI Methods*.

ACKNOWLEDGMENTS. We thank Hildegund Ertl and Hansjörg Hauser for the Ad.ckOVA-NP-GFP vector and the pStat1-eGFP vector, respectively, and Jonathan Kaye and Mark Greene for discussion of the experiments. This work was supported by National Institutes of Health/National Institute of Neurological Disorders and Stroke Grants 1U01 NS052465.01, 1R01-NS 057711, and 1R21-NSO54143 (to M.G.C.), and 1 R01 NS 054193 and R01 NS 42893 (to P.R.L); the Bram and Elaine Goldsmith and the Medallions Group Endowed Chairs in Gene Therapeutics (P.R.L. and M.G.C., respectively); the Drown Foundation; the Linda Tallen and David Paul Kane Foundation Annual Fellowship; and the Board of Governors at Cedars-Sinai Medical Center.

1. Stinchcombe JC, Griffiths GM (2003) The role of the secretory immunological synapse in killing by CD8+ CTL. *Semin Immunol* 15:301–305.
2. Poo WJ, Conrad L, Janeway CA, Jr. (1988) Receptor-directed focusing of lymphokine release by helper T cells. *Nature* 332:378–380.
3. Kupfer A, Mosmann TR, Kupfer H (1991) Polarized expression of cytokines in cell conjugates of helper T cells and splenic B cells. *Proc Natl Acad Sci USA* 88: 775–779.
4. Kupfer H, Monks CR, Kupfer A (1994) Small splenic B cells that bind to antigen-specific T helper (Th) cells and face the site of cytokine production in the Th cells selectively proliferate: Immunofluorescence microscopic studies of Th-B antigen-presenting cell interactions. *J Exp Med* 179:1507–1515.
5. Huse M, Lillemeier BF, Kuhns MS, Chen DS, Davis MM (2006) T cells use two directionally distinct pathways for cytokine secretion. *Nat Immunol* 7:247–255.
6. Huse M, Quann EJ, Davis MM (2008) Shouts, whispers and the kiss of death: Directional secretion in T cells. *Nat Immunol* 9:1105–1111.
7. Perona-Wright G, Mohrs K, Mohrs M (2010) Sustained signaling by canonical helper T cell cytokines throughout the reactive lymph node. *Nat Immunol* 11:520–526.
8. Barcia C, et al. (2006) In vivo mature immunological synapses forming SMACs mediate clearance of virally infected astrocytes from the brain. *J Exp Med* 203: 2095–2107.
9. Barcia C, et al. (2008) In vivo polarization of IFN-gamma at Kupfer and non-Kupfer immunological synapses during the clearance of virally infected brain cells. *J Immunol* 180:1344–1352.
10. Wiedemann A, Depoil D, Faroudi M, Valitutti S (2006) Cytotoxic T lymphocytes kill multiple targets simultaneously via spatiotemporal uncoupling of lytic and stimulatory synapses. *Proc Natl Acad Sci USA* 103:10985–10990.
11. Caramalho I, Faroudi M, Padovan E, Müller S, Valitutti S (2009) Visualizing CTL/melanoma cell interactions: Multiple hits must be delivered for tumour cell annihilation. *J Cell Mol Med* 13(9B):3834–3846.
12. Jenkins MR, et al. (2009) Visualizing CTL activity for different CD8+ effector T cells supports the idea that lower TCR/epitope avidity may be advantageous for target cell killing. *Cell Death Differ* 16:537–542.
13. Shamri R, et al. (2005) Lymphocyte arrest requires instantaneous induction of an extended LFA-1 conformation mediated by endothelium-bound chemokines. *Nat Immunol* 6:497–506.
14. Anikeeva N, et al. (2005) Distinct role of lymphocyte function-associated antigen-1 in mediating effective cytolytic activity by cytotoxic T lymphocytes. *Proc Natl Acad Sci USA* 102:6437–6442.
15. Yachi PP, Ampudia J, Zal T, Gascoigne NR (2006) Altered peptide ligands induce delayed CD8-T cell receptor interaction—a role for CD8 in distinguishing antigen quality. *Immunity* 25:203–211.
16. Jenkins MR, Tsun A, Stinchcombe JC, Griffiths GM (2009) The strength of T cell receptor signal controls the polarization of cytotoxic machinery to the immunological synapse. *Immunity* 31:621–631.
17. Anikeeva N, Sykulev Y (2011) Mechanisms controlling granule-mediated cytolytic activity of cytotoxic T lymphocytes. *Immunol Res* 51:183–194.
18. Fooksman DR, et al. (2010) Functional anatomy of T cell activation and synapse formation. *Annu Rev Immunol* 28:79–105.
19. Bergles DE, Diamond JS, Jahr CE (1999) Clearance of glutamate inside the synapse and beyond. *Curr Opin Neurobiol* 9:293–298.
20. Beal AM, et al. (2008) Protein kinase C theta regulates stability of the peripheral adhesion ring junction and contributes to the sensitivity of target cell lysis by CTL. *J Immunol* 181:4815–4824.